Analysis of non-linear plates by the boundary element method applied to concrete slabs

Gabriela R. Fernandes*, **Eduardo W. V. Chaves*** **& Wilson S. Venturini****

*Graduate Student; **Professor
São Carlos School of Engineering, University of São Paulo
Av. Carlos Botelho 1465, São Carlos, Brazil
e-mail: venturin@sc.usp.br

Key Words: Plate Bending, Boundary Elements and Non-linear Problems

ABSTRACT

Abstract. *Analysis of plate bending problems based on classical Kirchhoff's hypothesis and using BEM formulations has already demonstrated to be efficient and accurate. In this work the BEM non-linear formulation for Kirchhoff plates in bending applied to model reinforced concrete elements is discussed. The integral equations of displacements, bending and twisting moments and shear forces are derived and modified properly to give numerical algorithm to model non-linear behaviours. A simple and specific plastic criterion appropriate to model reinforced concrete slabs is proposed, in which concrete in compression is governed by the Mises surface, while no-tension is adopted for the traction zone. Then, the Mazars continuum damage model is also implemented to better consider tension stiffness effects. For the proposed formulation, the internal forces are approached by numerical integrals along the plate thickness. A Gauss scheme was conveniently employed to achieve the total internal force values after verifying the non-linear criterion at each basis as well.*

1 INTRODUCTION

The boundary element method (BEM) is already a well-established numerical technique to deal with an enormous number of engineering complex problems. Among them, plate-bending analysis has attracted the attention of many researchers during the last years proving to be a particularly adequate field of applications for that technique. For instance, BEM is particularly suitable to evaluate internal force concentrations due to point loads, that very often occur in this kind of structures. Thin and moderately thick plates in bending exhibit concentration of bending and twisting moments and shear forces either in the vicinity of concentrated loads or due to loads distributed over small regions. Line loads due to the presence of walls or reactions of linear supports cause high effort gradients as well. Moreover, BEM can deal with deflections, slopes, moments and shear forces approaching them by using the same order polynomials. Thus, shear efforts, for instance, are better evaluated when compared with other numerical method solutions; it depends only on the assumed boundary value approximation.

Since 1978, when a first general direct formulation based on the Kirchhoff's hypothesis has appeared, the technique has experimented a rather large growth, being nowadays applied to several practical engineering problems. The first works discussing the use of boundary element direct formulation, in conjunction with the Kirchhoff's theory, are due to Bezine[1,2], Stern[3] and Tottenhan[4]. It is also important mentioning some previous works, dealing with plate bending problems as well, but in the context of indirect methods[5,6,7]. Those works, as well as several other more recent publications, have pointed out the capability of the method to model plates in bending, taking into account its accuracy and confidence. For instance, Gou-Shu[8] and Hartmann & Zotemantel[9] have presented interesting approaches, where displacement restrictions at internal points and the use of hermitian interpolations were discussed in details. Venturini & Paiva[10] have shown several alternatives to define the algebraic system of equations by placing the collocations either along the boundary or at particular outside points.

The works reported above basically describe formulations of the BEM linear plate bending problem, for which the Kirchhoff hypothesis has been assumed, and their applications in engineering. After commenting those works, other developments must be point out for a wider overview concerning the general use of BEM to deal with plate bending problems. For instance, it is important to mention the plate bending formulation proposed, in 1982, to deal with moderate thick plates[11] by incorporating the Reissner's hypothesis[12]. BEM formulations related with plate bending analysis for problems where large displacement assumptions must be taken into account have also appeared in several works. Kamiya & Sawary[13] have proposed a so-called DBEM direct formulation for finite deflections of thin plates; Tanaka[14] has developed a coupled boundary and inner domain integral equations written in terms of stresses and displacements.

In order to deal with two-dimensional elastoplastic problems using boundary elements, Telles & Brebbia[15], in 1980, have proposed an efficient scheme based on the initial stress technique. For elastoplastic plate bending analysis, considering the Kirchhoff theory and using BEM, we can mention the work due to Moshaiov & Vorus[16], in which a particular incremental scheme has been proposed. Chueiri & Venturini[17] have also studied this problem introducing particular models to deal with concrete slabs. Non-linear boundary element models have been also developed to deal with thick plates by taking into consideration the Reissner's theory (e.g. Ribeiro & Venturini[18] and Karan & Telles[19]) More recently, a book containing many works dedicated to non-linear thin and moderate thick plates has been published[20].

In the present paper, boundary element formulations for Kirchhoff's plates in bending are proposed to deal with non-linear problems, particularly to model non-linear reinforced concrete slabs, using elastoplastic and continuum damage models. Integral representations of displacements, bending and twisting moments and shear forces will be derived from the Betti's reciprocal work theorem, taking into account an initial moment field applied over the non-linear region. From those integral representations, i.e., displacement, moment and shear force equations, the BEM non-linear formulation for the Kirchhoff plate-bending problem is introduced.

The formulation is first derived to deal with problems governed by constitutive law of moment $\times$ curvature type, then extended to incorporate layered models, where the initial moment fields are evaluated by numerical integrals along the plate thickness. The

concrete behaviour is assumed governed by plastic or continuum damage models, given in terms of stresses and verified at Gauss points taken along the plate thickness. A particular plastic model, assuming the Mises surface with tension cut off, appropriate to represent reinforced concrete slab behaviour was implemented. In order to represent better tension stiffness effects, the Mazars continuum damage model was also implemented. The reinforcement, for which elastoplastic behaviour has been assumed, was independently verified at the actual reinforced positions.

Two different schemes to model concrete slabs are discussed. A very simple procedure is initially considered, where the neutral axis is assumed to lay on the plate middle surface. Then, the model is improved leading to the second alternative, now including a scheme to define properly the neutral axis position, enforcing no in plane stress resultant.

After implementing those numerical models, derived from the varying thickness plate and the non-linear formulations, some examples are taken to illustrate the accuracy of the proposed schemes.

2 BASIC EQUATIONS

A flat plate of thickness t, referred to a Cartesian system of co-ordinates with axes x_1 and x_2 laying on its middle surface and axis x_3 perpendicular to that plane, is considered. It is assumed that the plate supports distributed load g acting in the x_3 direction on the plate middle plane, in absence of distributed external moments. For this plate, the equilibrium equations are given by the following differential expressions:

$$m_{ij,j} - q_i = 0 \quad \text{and} \quad q_{i,i} + g = 0 \tag{1a, b}$$

where m_{ij} are bending and twisting moments and q_i represents shear forces, with the subscripts defined in the range i,j={1, 2}.

Equations (1) can be joined together to give the well known plate bending differential equation written in terms of moments:

$$m_{ij,ij} + g = 0 \tag{2}$$

The plate domain, defined over the middle surface, is denoted by Ω###, while its boundary is represented by Γ. Along Γ, the following generalised boundary conditions may be assumed: $u_i = \bar{u}_i$ on Γ_1 and $p_i = \bar{p}_i$ on Γ_2, where $\Gamma_1 \cup \Gamma_2 = \Gamma$. The generalised displacements u_i are deflections, w, and rotations, $\partial w/\partial n$, while generalised tractions are given by normal bending moments, M_n, and effective boundary shear forces, V_n.

Let us now summarise the basic relations of plate bending based on the Kirchhoff's theory to deal with non-linear strain problems. For simplicity, as usual the total strain components can be divided into two parts, as follows:

$$\varepsilon_{ij} = \varepsilon_{ij}^e + \varepsilon_{ij}^p \tag{1}$$

where ε_{ij}^e and ε_{ij}^p are the elastic and plastic strain parts, respectively.

The strain components can be associated with the deflection derivatives, $w_{,ij}$, i.e., with the middle surface curvatures. By using the Hooke's law and performing the appropriate stress integrals along the plate thickness, the total moment components can be obtained:

$$m_{ij} = m_{ij}^{e} - m_{ij}^{p} \tag{2}$$

or

$$m_{ij} = -D\left[\nu w_{,kk}\,\delta_{ij} + (1-\nu)w_{,ij}\right] - m_{ij}^{p} \tag{3}$$

in which δ_{ij} is the Kronecker delta, υ is the Poisson's ratio and the classical plate stiffness D is given by: $Et^3/\left[12(1-\nu^2)\right]$, with E being the Young's modulus.

The equilibrium conditions of an infinitesimal plate element give the following differential equations written in terms of moments and shear forces:

$$m_{ij,i} - q_j = 0 \quad \text{and} \quad q_{i,i} + g = 0 \tag{4a,b}$$

By differentiating equation (3) and then replacing it into equation (4a), one can write shear forces in terms of deflection derivatives, as follows:

$$q_j = -Dw_{,kkj} - m_{ij,i}^{p} \tag{5}$$

Replacing equation (4b) into (4a) and then using equation (3), one can achieve the equilibrium final expression, for plates with constant stiffness D, written in terms of displacements:

$$w_{,iijj} = \left(g - m_{ij,ij}^{p}\right)/D \tag{6}$$

where $w_{,iijj} = \nabla^2 w$, stand for the Laplacian operator here applied on deflections w.

Equation (6) is the final differential equation that governs a plate over which an initial moment field, here particularised to the plastic moment field m_{ij}^{p}, is applied. This loading is appropriate to analyse structures subjected to temperature changes, to consider material shrinkage, as well as to model other material non-linear behaviours.

It is worth remembering that due to the assumed Kirchhoff hypothesis only four boundary values are independent: twisting moments and the shear force along the boundary have to be combined together to give the well-known boundary value, the effective shear force, as follows:

$$V_n = q_n + \partial m_{ns} / \partial x_s \tag{7}$$

where (n, s) are the local co-ordinate system, with n and s referred to the boundary normal and tangential directions, respectively; no summation is implied.

3 INTEGRAL REPRESENTATIONS

As it is well known, the direct formulation of the boundary element method for Kirchhoff's plates can be derived from a reciprocity relation written in terms of bending moments and curvatures of two independent mechanical states. The first state is represented by the actual plate bending problem valid over the domain Ω, for which

curvatures $w_{,ij}(q)$ and elastic moments $m^e_{ij}(q)$ at a field point q are defined, as well as the associated boundary values: two generalised displacements, $u_i(Q)$, and two generalised tractions, $p_i(Q)$, referred to a boundary field point Q.

The second elastic state is given by the well known fundamental solution $w^*(s,q)$, the deflection at the field point q due to an unit load applied at a source point s. This elastic state is defined over the infinite space of domain Ω_∞ that contains Ω (see figure 1). From this state, fundamental values for curvatures, $w^*_{,ij}(s,q)$, and moments, $m^*_{ij}(s,q)$ can be easily derived (see appendix). Taking into account both states and assuming that the stiffness D is constant, the following reciprocity relation is easily found:

$$\int_\Omega m^*_{ij}(s,q)\,w_{,ij}(q)\,d\Omega(q) = \int_\Omega m^e_{ij}(q)\,w^*_{ij}(s,q)\,d\Omega(q) \tag{11}$$

After replacing the elastic moment value, $m^e_{ij}(q)$, in the last integral of equation (11), one can write the standard the reciprocity relation usually adopted to deal with temperature or non-linear problems based on the initial moment technique, as follows[17]:

$$\int_\Omega m_{ij}(q)\,w^*_{,ij}(s,q)\,d\Omega(q) = \int_\Omega m^*_{ij}(s,q)\,w_{,ij}(q)\,d\Omega(q) - \int_\Omega w^*_{,ij}(s,q)\,m^o_{ij}(q)\,d\Omega(q) \tag{12}$$

From equation (12), it is very easy to derive the integral representation of displacements, as well the other integral equations usually required to solve a plate bending problem. For a plate subjected to a transversal load g(q) applied over a particular region Ω_g, one can derive the following deflection integral representation:

$$C(S)w(S) + \int_\Gamma \left(V^*_n(S,Q)w(Q) - M^*_n(S,Q)\frac{\partial w}{\partial n}(Q) \right) d\Gamma(Q) + \sum_{C=1}^{N_c} R^*_C(S,C)w_C(C) =$$

$$= \int_\Gamma \left(V_n(Q)w^*(S,Q) - M_n(Q)\frac{\partial w^*}{\partial n}(S,Q) \right) d\Gamma(Q) + \sum_{C=1}^{N_c} R_C(C)w^*_C(S,C) +$$

$$+ \int_{\Omega_g} \left(g(q)w^*(S,q) \right) d\Omega(q) - \int_\Omega w^*_{,k\ell}(S,q)\,m^p_{k\ell}(q)\,d\Omega(q) \tag{13}$$

where Q and q are field points taken along the boundary Γ and inside the domain respectively, while s is source point that can be placed anywhere.

In equation (13), w, $\partial w/\partial n$, M_{nn}, V_n and R_C are actual plate boundary values, deflections, rotations, normal bending moment, effective shear forces and corner reactions, respectively. The values indicated by * are the corresponding ones derived from the infinite domain problem with the source point defined inside the domain, outside or along the boundary. C(S) represents the well known free term that is equal to the unit when S is an internal point, zero when outside defined and $\beta_C/2\pi$ for boundary points, being β_C the internal angle at S.

From equation (13) one can derive slope, moment and shear force integral representations by differentiating it and applying appropriately the Hooke's law. Using either equation (13) or any other integral representation derived from it is enough to

establish a set of algebraic equations to solve the problem. As two boundary values are unknown at each node, two corresponding relations must be written. In order to use only deflection representations, defining two collocation points for each discretization node is required, as well as another integral representation corresponding the extra node defined at geometrical corners[10] to guarantee displacement and reaction independent values at these nodes. It is important to stress that one can find the second algebraic representation for each node using any other representation obtained from equation (12). Adopting deflection and slope representations is the usual way followed to solve plate bending problems by BEM[1,2,3,4].

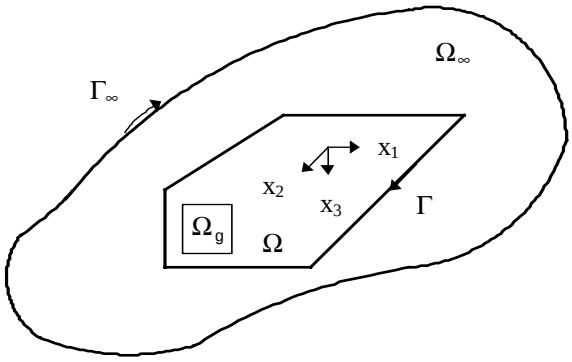

Figure 1. Plate domain inserted into the infinite space

Moment and shear force integral representations for internal points (therefore assuming C(S)=1) can be derived from equation (13) by carrying out its second and third derivatives and applying appropriately internal force definitions given in equations (3) and (5), respectively. One must pay attention how to carry out those derivatives; for any case, free terms will appear when performing derivatives of singular integral terms. By differentiating equation (13) twice and introducing the definitions given by equation (3), one obtains,

$$m_{ij}(s) = -\int_{\Gamma}\left[V^{*}_{nij}(s,Q)w(Q) - M^{*}_{nij}(s,Q)\frac{\partial w}{\partial n}(Q)\right] - \sum_{c=1}^{N_c} R^{*}_{cij}(s,Q)w_c(Q) + \sum_{c=1}^{N_c} w^{*}_{cij}(s,Q)R_c(Q)$$
$$+\int_{\Gamma}\left[w^{*}_{nij}(s,Q)V_n(Q) - \frac{\partial w^{*}_{ij}}{\partial n}(s,Q)M_n(Q)\right]d\Gamma(Q) + \int_{\Omega_g} w^{*}_{ij}(s,q)g(q)d\Omega(q)$$
$$-\int_{\Omega} e^{*}_{,ijk\ell}(s,q)m^{p}_{k\ell}(q)d\Omega(q) - g_{ijk\ell}(q)M^{p}_{k\ell}(q) - m^{p}_{ij}(q) \qquad (14)$$

In equation (14), all kernels are derived from second derivatives of the fundamental values used in equation (13). They are easily achieved from $V^{*}_{n}(q,P)$,

$M^*_n(q,P)$, $R^*_c(q,P)$, $w^*_c(q,P)$, $w^*(q,P)$, $\partial w^*(q,P)/\partial n$ and $w^*_{,k\ell}(q,P)$, applying the following operator,

$$-D\left[\nu\delta_{ij}\frac{\partial^2(q,P)}{\partial x_k\partial x_k}+(1-\nu)\frac{\partial^2(q,P)}{\partial x_i\partial x_j}\right] \tag{15}$$

Note that the last domain integral in equation (14) exhibits singularity of order $1/r^2$, given by the kernel $e^*_{ijk\ell}(q,P)$, requiring therefore proper care to be evaluated. As adopted to obtain the other kernels above, $e^*_{ijk\ell}(q,P)$ can be easily found by applying the operator (15) to $w^*_{,k\ell}(q,P)$. The free term of equation (14), resulting of differentiating a singular integral term, is given by,

$$g_{ijk\ell}(q)=-\tfrac{1}{8}\left[(1-\nu)(\delta_{ik}\delta_{\ell j}+\delta_{kj}\delta_{i\ell})+(1+3\nu)\delta_{ij}\delta_{k\ell}\right] \tag{16}$$

Following the same steps used to achieve the integral equation (14), one can also derive the integral representation of shear forces. After differentiating equation (13) three times and applying the shear force definition, equation (5), one obtains,

$$q_\beta(s)=-\int_\Gamma\left[V^*_{n\beta}(s,Q)w(Q)-M^*_{n\beta}(s,Q)\frac{\partial w}{\partial n}(Q)\right]d\Gamma(Q)$$

$$-\sum_{c=1}^{N_c}R^*_{c\beta}(s,Q)w_c(Q)+\sum_{c=1}^{N_c}w^*_{c\beta}(s,Q)R_c(Q)+\int_\Gamma\left[w^*_\beta(s,Q)V_n(Q)\right.$$

$$\left.-\frac{\partial w^*_\beta}{\partial n}(q,P)M_n(P)\right]d\Gamma(P)+\int_{\Omega_g}w^*_\beta(q,p)g(p)d\Omega(p)$$

$$-\int_\Omega e^*_{,\beta k\ell}(q,p)m^p_{k\ell}(p)d\Omega(p)-\bar{q}^p_\beta(q) \tag{17}$$

Equation (5) can be used to achieve an operator similar to the one given by equation (15), now based on the third derivatives of original kernels of equation (13), as follows:

$$-D\frac{\partial^3}{\partial x_m\partial x_m\partial x_\beta} \tag{18}$$

Applying the operator (18) to the kernels of equation (10) one obtains $V^*_{n\beta}(q,P)$, $M^*_{n\beta}(q,P)$, $R^*_{c\beta}(q,P)$, $w^*_{c\beta}(q,P)$, $w^*_\beta(q,P)$, $\partial w^*_\beta(q,P)/\partial n$ and $e^*_{,\beta k\ell}(q,P)$.

The free term in equation (17), appeared due to the order of the present singularities and also representing the discontinuity of integral representation, is given by,

$$g_\beta(q)=-\tfrac{1}{2D}\frac{\partial}{\partial x_\beta(q)}M^p_{kk}(q) \tag{19}$$

In this work, equations (13), (15) and (17) are adopted to analyse non-linear plate bending problems. For this case, the moment values at internal points must be defined as

problem unknowns, requiring therefore three extra equations for each domain node. In the next sections, those integral equations are transformed into algebraic representations to build appropriate schemes to deal with non-linear plate bending problems.

4 BEM ALGEBRAIC EQUATIONS FOR VARYING THICKNESS PLATES

As usual for any BEM formulation, the integral representations (13), (15) and (17), can be transformed into algebraic expressions after discretizing the boundary into elements, the domain into cells and approaching appropriately boundary and internal values. For the present case, the plate boundary has been discretized into geometrically linear elements over which the boundary values have been approximated by quadratic shape functions. Over the domain, the initial moments or the moment plastic parts, $m_{ij}^{p}(q)$, are approximated as well, now adopting linear shape functions defined over triangular cells.

The approximations of the boundary and internal values enable us to write algebraic representations of deflections, rotations, moments and shear forces for any collocation point taken inside the domain, along the boundary or even out of the plate, using the integral expressions derived in the last section. After selecting an appropriate number of algebraic equations, one can assemble a convenient set of equations to solve the problem in terms of boundary values. Note that there are four boundary values at each node defined by the discretization, plus two extra values at each corner to take into account corner reactions. As it has already been observed in previous studies[10], it is better to use only deflection representations to define the final set of equations, taking the collocation points either along the boundary or outside the body. It is worth noting that moment algebraic equations written for collocations defined inside the domain are also required to complete the total amount of relations to solve non-linear plate bending problems. Deflection and shear force algebraic equations at internal points are written only for the result output if required.

Although other alternatives concerning the collocation point selection may be proposed to achieve the appropriate algebraic representations, two strategies have been tested and proved to give accurate results. The first scheme consists of defining one collocation point coincident with the boundary node (Q) and another one (A) externally placed at a convenient small distance d from the boundary. For the second strategy, two outside collocation points (A1 and A2) are adopted, as shown in Figure (2). Defining two independent boundary collocation points for each node is possible, but this strategy leads to singular systems of equations; it can be adopted, however if at least one external collocation is defined to guarantee that the algebraic equations are linearly independent.

As a rule, continuous elements are adopted to keep boundary value continuity between boundary elements, but discontinuities are assumed at corners and at other points where boundary conditions may change abruptly. For those cases, it is convenient to define five collocation points associated with five unknowns (ten boundary values: w, $\partial w/\partial n$, V_n and M_n related to the adjacent element ends plus w_c and R_c, the corner values). Four collocations points are related with the element end unknowns, while the extra collocation makes corner reactions and displacements independent values.

Figure 2 illustrates the strategies described above to select the collocation points. The distance d_i is given by: $d_i = a_i \ell_m$, being ℓ_m the average adjacent element length and a_i a parameter defined within the range {0.1, 0.5} for both collocation point selection

schemes described above. A sub-element technique is always required to perform accurately the integrals along the adjacent elements.

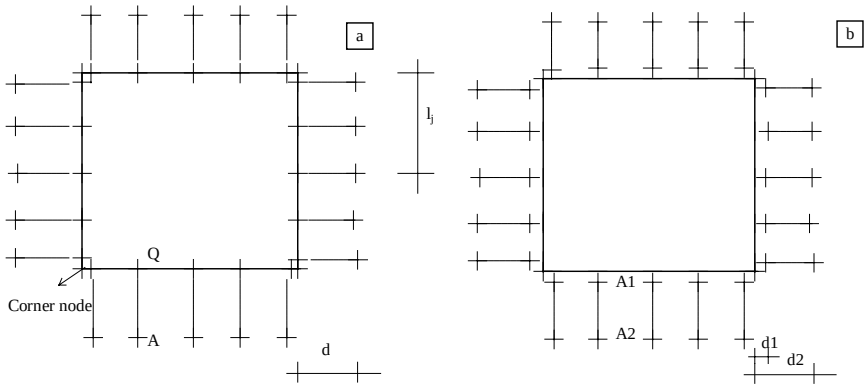

Figure 2: Boundary discretization and collocation point selection;
a) collocations defined along the boundary; b) outside collocations only.

In order to perform the integrals over internal cells, they have been transformed to its boundary. This transformation is locally performed for each cell, leading therefore to three integrals along the cell sides. Those integrals are then performed adopting the same sub-element technique used to obtain the boundary matrices **H** and **G**. to be accurate.

Writing the discretized form of equation (13), for the necessary number of collocation points, one finds the BEM classical matrix equation, now including the influence due to the initial moment field, or plastic moments, as follows[17],

$$\mathbf{HU} = \mathbf{GP} + \mathbf{T} + \mathbf{EM}^{\mathrm{p}} \tag{20}$$

Vectors **U** and **P**, in equation (20), contain the generalized displacement and traction nodal values; vector **T** represents the loading and $\mathbf{M}^{\mathrm{p}}$ contains plastic moments at internal and boundary nodes. **H** and **G** are the standard square matrices achieved by integrating all boundary elements, while **E** is a matrix obtained by performing the integrals over all cells.

Following the same steps used to write equation (20), moment and shear integral representations, equations (150 and (17), can also be written into their algebraic form,

$$\mathbf{M} = -\mathbf{H}'\mathbf{U} + \mathbf{G}'\mathbf{P} + \mathbf{T}' + (\mathbf{E}' - \mathbf{I})\mathbf{M}^{\mathrm{p}} \tag{21}$$

$$\mathbf{Q} = -\mathbf{H}''\mathbf{U} + \mathbf{G}''\mathbf{P} + \mathbf{T}'' + \mathbf{E}''\mathbf{M}^{\mathrm{p}} \tag{22}$$

with **I** being the identity matrix;

All matrices appearing in equations (21) and (22) are similar the ones in equation (20), obtained by using the corresponding kernel exhibited in equations (15) and (17).

As usual in non-linear boundary element formulations[15,17,18], the matrix equations (20), (21) and (22) can be conveniently arranged to express the solution in terms of boundary values, moments and shear forces, as follows,

$$\mathbf{X} = \mathbf{L} + \mathbf{RM}^{\mathrm{p}} \quad \mathbf{M} = \mathbf{N} + \mathbf{SM}^{\mathrm{p}} \quad \mathbf{Q} = \mathbf{N}' + \mathbf{S}'\mathbf{M}^{\mathrm{p}} \tag{23a,b,c}$$

In equations (23) **L**, **N** and **N'** give the elastic solution due to prescribed loads acting along the boundary or over the domain, while the $\mathbf{M}^{p}$ effects are represented by the matrices **R**, **S** and **S'**.

5 NON-LINEAR PLATE BENDING PROBLEMS

As it has already been said, equations (23) can be adopted to model non-linear behaviours when initial moment fields can be computed from the adopted plastic criterion. For any elastoplastic analysis, general relations between stress and strain must be specified to govern the elastic and plastic behaviours and also to indicate the onset of plastic flow. For simplicity, instead using a model defined in terms of stresses, one can adopt simple criteria based on moment components and the hardening parameter k. Chueiri & Venturini[17] have presented a simple BEM procedure to model plastic behaviour of plates governed by a global constitutive relation written in terms of moments and curvatures. In this case, the plastic surface is expressed by:

$$F(m_{ij}, k) = f(m_{ij}) - m_y(k) = 0 \tag{24}$$

where $f(m_{ij})$ represents an equivalent moment and $m_y(k)$ is the yielding moment which depends on the equivalent plastic curvature, $1/r$.

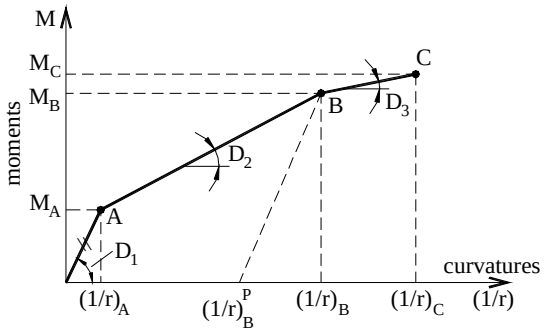

Figure 4. Three-linear moment curvature diagram

One possibility of constructing an elastoplastic model to be joined to a BEM code can be found in the work written Chueiri & Venturini[17]. For this model, the three-linear moment × curvature diagram, Figure 4, was assumed to represent the reinforced concrete behaviour subjected to simple bending. This moment × curvature relation is very similar to the one recommended by CEB-FIP[21]. Von Mises yield surface within the concept of associate plasticity was assumed to complete plastic model, giving therefore the plastic curvatures.

Although the model described above is adequate to represent concrete behaviour, analysing concrete slabs could be improved by considering the proper material behaviour through the thickness. Here, a more general model will be discussed and implemented not only applied plastic plate problems, but also to model concrete slabs, for which continuum damage mechanics behaviour is assumed. Thus, in order to define a general

non-linear model (plasticity and continuum damage models) the plate can be assumed divided into layers, that can exhibit different properties[22,23].

By following this strategy, each layer is characterised by having its own material and constitutive model. Stresses are computed at layer middle points and assumed constant through the layer thickness t_n. Any stress distribution through the thickness can be represented by constants rectangles (see Figure 5). In this work, this technique is modified a little bit, to consider any distribution, stresses for instance, approximated along the plate thickness by polynomials. In fact, there is no need to define the stress distribution shape along the thickness. During the non-linear process only bending moments and normal forces, given by stress integrals through the plate thickness, are required. One can, therefore, perform those integrals using numerical gaussean schemes. Using that scheme, material properties and the stress values must be specified only at known stations. The number of stations to perform the integrals and their homogenous co-ordinate ζ_n are chosen according to the convenient Gauss scheme to be adopted. Reinforcement is considered as additional terms with their co-ordinates previously defined. Strain values always follows the Bernouille-Navier rules, while stresses are governed by the assumed material criterion

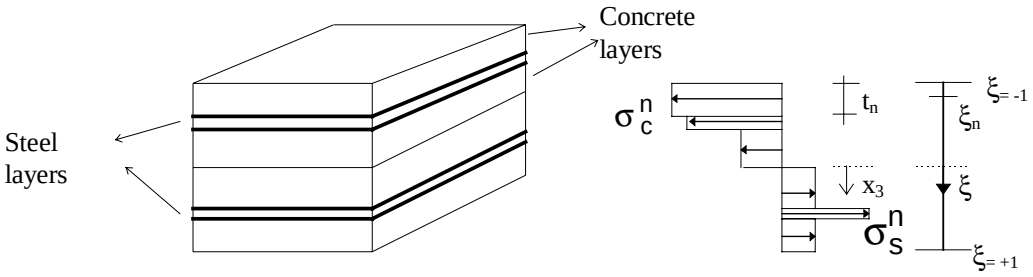

Figure 5: Stratified Model for the reinforced concrete

Bearing in mind that throughout the non-linear iterative scheme the stress distribution σ_c along the plate thickness t has no defined shape (it will depend on the adopted Gauss point number N_g), moment components have to be evaluated by performing numerically the corresponding integrals given by:

$$m_{ij} = \int_{-t/2}^{t/2} \sigma_{ij}^{c} x_3 dx_3 + \sum_{k=1}^{Ns} \delta_{ij} \sigma_{ij}^{sk} A_{sk} x_{3sk} \tag{25}$$

where σ_{ij}^{sk} is the steel stress of a layer placed at x_{3sk}, in direction x_1 or x_2, while A_{sk} represents the steel bas cross section, N_s is the reinforced layer number and δ_{ij} is the Kronecker delta.

Computing the integral in equation (25) by using a Gauss scheme, one has:

$$m_{ij} = = \frac{t^2}{4} \sum_{IG=1}^{Ng} \sigma_{ij}^{c} \xi_{IG} W_{IG} + \sum_{k=1}^{Ns} \delta_{ij} \sigma_{ij}^{sk} A_{sk} x_{3sk} \qquad (i, j = 1, 2) \tag{26}$$

Equation (26) is used to compute the internal moment tensor, for a specific plate cross section. This value is computed assuming the plate middle surface to define the neutral axis, therefore dealing with a symmetric stress distribution diagram. For concrete slabs, one must take into account that the material behaves differently when in tension or in compression. In addition, reinforcement is usually non-symmetrically distributed. Thus, the neutral axis is no longer defined by the middle surface. In order to continue the analysis in the context of simple bending, one needs to define the new position of the neutral axis enforcing the stress resultant to be zero. This is made separately for each moment component. Assuming three independent curvature components one can compute the corresponding normal forces by integrating separately the three stress component distributions. An iterative procedure where the neutral axes are searched must be adopted to enforce the three normal force components to be zero together. After achieving this equilibrium, the moment values can be computed.

The iterative process consists of assuming that the neutral axis new position can be estimated by linear interpolation. The normal forces are computed in the same similarly to the moment values, i.e. integrating numerically the stress distribution along the cross section. In fact, the expressions are similar to equations (25) and (26) suppressing the livers x_3 and x_{3sk}. Using two previous computed values for the normal forces n_{1i} and n_{2i}, the next value of the neutral axis position, z_i, is approached by:

$$z_i = z_{2_i} + \frac{n_{2i}\left(z_{1i} - z_{2_i}\right)}{n_{2i} - n_{1i}} \tag{27}$$

where z_{1i} and z_{2i} are previous positions used to compute n_{1i} and n_{2i}, respectively.

After approaching z_i, we are able to obtain the strain increments due to the neutral axis change and consequently the total stresses required to compute the actual moment values.

As the plate behaviour was assumed non-linear, an incremental and iterative procedure, as the procedure described bellow, must be adopted to analyse plates in bending. First, we have to choose previously a tolerance to clear define the iterative procedure end for a particular increment. For any iteration “j” inside a load increment “i” one has to start by computing the elastic moment increments $\Delta\mathbf{M}^{\mathbf{e}}$, for all boundary and domain nodes, using one of the following expressions:

$$\left\{\Delta\mathbf{M}^{\mathbf{e}}\right\}_{\mathbf{i}}^{\mathbf{1}} = \beta_{\mathbf{i}}\{\mathbf{N}\} \qquad \text{if} \quad j = 1 \tag{28a}$$

$$\left\{\Delta\mathbf{M}^{\mathbf{e}}\right\}_{\mathbf{i}}^{\mathbf{j}} = [\mathbf{S}]\left\{\Delta\mathbf{M}^{\mathbf{p}}\right\}_{\mathbf{i}}^{\mathbf{j-1}} \qquad \text{if} \quad j \geq 2 \tag{28b}$$

In equations (28a) β_i is the load factor, $\mathbf{N}$ and $\mathbf{S}$ are given by (23) and $\Delta\mathbf{M}^{\mathbf{p}}$ is the plastic moment increment computed during the previous iteration, even when it was performed during the increment i-1.

At that point one needs to compute the actual moment field taking into account particular criteria for each concrete layer and for the reinforcement as well. Using the Hooke’s law, the corresponding curvature increment is evaluated from the elastic moment increment. Then, at each Gauss point and at the reinforcement positions, strain and stress elastic increments are computed. As superposition is admitted, those values can be accumulated at proper vectors. For concrete material, verified only at Gauss points, the

tensile stresses are neglected. This correction is applied to the total stress vector before verifying the assumed constitutive model. For simplicity and due to its yielding surface be a rather similar to the Kupfer model[25] in compression, Von Mises criterion was adopted together with softening stress × strain curves. For the reinforced layer the steel behaviour is given by a uniaxial elastoplastic curve exhibiting hardening effects.

After verifying the non-linear model at all Gauss points and reinforcement layers, we are able to compute the three components of the normal force resultants, n_x, n_y and n_{xy}. Then, the neutral axes are approached enforcing these components to be zero, following the iterative scheme already previously described. After finding the actual strain distribution throughout the plate thickness, the true moment and true moment increment ($\Delta\mathbf{M}^{V}$) vectors are evaluated, equation (26). The plastic moment increments are then computed at all boundary and internal nodes:

$$\left\{\Delta\mathbf{M}^{p}\right\}_{i}^{j+1} = \left\{\Delta\mathbf{M}^{e}\right\}_{i}^{j} - \left\{\Delta\mathbf{M}^{v}\right\}_{i}^{j} \tag{29}$$

This corrector value $\left\{\Delta\mathbf{M}^{0}\right\}_{i}^{j+1}$ has to be applied to the plate to establish again the equilibrium, equation 28b. This iterative scheme continues until the corrector vector could be neglected according a tolerance previously defined.

After the increment end, where the structure equilibrium is achieved, it is possible to compute other values not required during the iterative process. So, boundary values and shear forces can be evaluated using expressions (23).

For damage analysis, the same procedure is followed, replacing plastic values by damaged values and adopting the appropriate criteria to define the true values at each Gauss point. Note that the tensile stresses are no longer neglected; a particular behaviour is now assumed for the tensile region.

6 NUMERICAL EXAMPLES

In this section, two numerical examples have been chosen to illustrate the layered BEM approach model proposed to simulate non-linear plates in bending, particularly, examples of concrete slabs are discussed here.

For those two examples the layered model has been successfully applied. The scheme adopted to perform the integral along the thickness to compute plate internal forces has been verified, showing that a reasonable reduced number of stations for the Gauss procedure is enough to obtain good quality results. The proposed plastic scheme based on the application of the modified von Mises at each station defined along the thickness proved to be appropriate to be used together with BEM to model reinforced concrete. The continuum damage behaviour, simulated by the four parameter model proposed by Mazars[29,30], showed to be applicable together with BEM to model concrete slabs as well. This model has also been implemented following the non-linear formulation presented in the last section. Some modifications have to be made in the non-linear algorithm to take into account the damage model and its intrinsic variables. For instance, no irreversible strain is assumed for this simplified model; after cracking one has to model the plate stiffness reduction during either loading or unloading processes. Thus, the algorithm was little modified to use strains as the guide variable.

In the first example, the plate geometry and boundary conditions are particularly defined in order to simulate the behaviour of a 30cm thick beam (t=30cm), as shown in figure 10. The applied load is given by the moment M = 500kNcm, distributed along the simply supported sides of length 2b=20cm.The other two sides of length equal to 2a=150cm are free, with no prescribed displacement or rotation. The boundary was discretized into 8 quadratic elements, while the domain initial moments are approached over 24 cells, which require the definition of 5 internal points, as shown in the figure 11. The refinement is constant and displayed only in the x_1 direction. For the concrete material, elastic modulus E_c was assumed equal to 3000kN/cm^2, while the Poisson ration ν=0 was taken. The concrete ultimate stress, f_c=3kN/cm^2 was adopted, with softening modulus equal to 1500kN/cm^2. The steel elastic modulus E_s was assumed equal to 27000kN/cm^2, with hardening modulus K_s=14000kN/cm^2, while the bar cross section taken was A_s=0.5cm^2/cm. All bars have been placed at x_3 = 12cm. The plastic criterion for the reinforcement was defined by the yield stress σ_y=24kN/cm^2, with no hardening or softening. The convergence was controlled by a tolerance of 0,1%.To run this example two outside collocation points where adopted; they are specified by their distance to the boundary, a_1=0.1 and a_2=0.25.

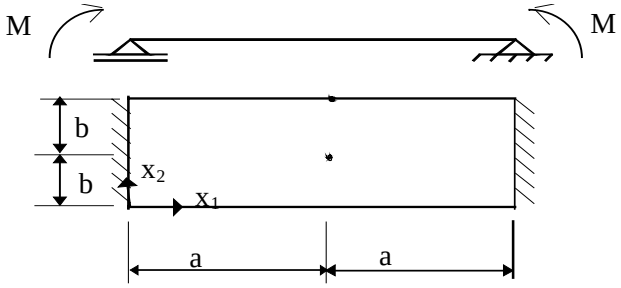

Figure 10. Beam definition

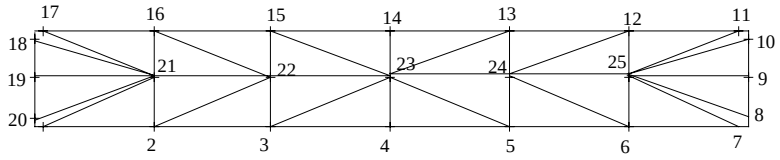

Figure 11. Plate discretization

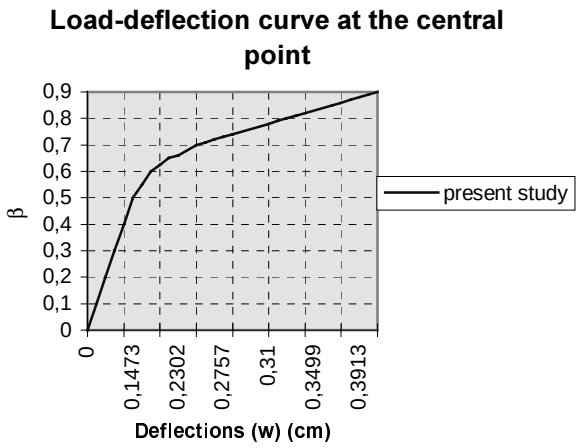

Figure 12. Load-deflection curve at the central point

The load has been applied in 30 increments. Elastic responses were observed until the load factor β reached 0.55. Plastic strains appeared in the steel bat for β equal to 0.60, while yielding was observed in the concrete region only for $\beta > 0.77$. The analysis stopped at $\beta=0.91$, when the assumed concrete maximum deformation of 0.003 was reached.

Table 1 gives moments in the x_1 direction and deflections for $\beta=0.9$ (see also figure 13). Deflections computed at the plate middle point (23), during the incremental process, are displayed in the figure12, while the final values ($\beta=0.90$) captured along x_1 are given in figure 13. The same results have also been achieved by analysing the corresponding non-linear beam.

Table 1. Final deflections w and bending moments M_{x1}

Node	M_{X1} (kNcm)	w(cm)
1	449.83	
2	449.43	
3	449.69	
4	448.83	
19	449.95	0
20	449.95	
21	449.99	0.2272
22	450.38	0.3635
23	450.69	0.4090
24		0.3635
25		0.2272

In the second example taken to show the proposed formulation, a square plate (a = 36”), with thickness t = 5,5” and simply supported along all sides, is analysed, assuming that a nearly concentrated load is applied at its centre (see figure 14). To run the example the load was assumed to be spread over the area 10”×10” resulting into g=800psi. The

plate boundary was also discretized into 8 quadratic elements and the domain into 32 cells, with 9 internal points, as shown in figure 15. A finer mesh with 16 elements, 128 cells, 36 boundary nodes and 49 internal points were also used to check the plastic solution. The same reinforcement is displayed in both directions, x_1 and x_2. The steel elastic modulus E_s=30000000psi was adopted, together with hardening modulus k=0., cross section A_s=0.04455in^2/in, yield stress σ_y=44000psi and bar position at x_3 = 1.75". The concrete is characterised by its elastic modulus E_c equal to 4000000psi, Poisson ratio ν=0.15, the ultimate strength f_c=6920psi and softening modulus 5448819psi. The analysis has been carried out using two outside collocation points specified by their distance to the boundary, a_1=0.1 and a_2=0.25. A tolerance of 0,1% was assumed to govern the convergence criterion, while only 8 Gauss points showed to be enough to perform the integrals across the slab thickness.

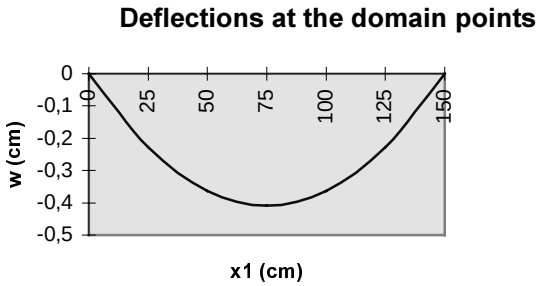

Figure 13. Deflections at the domain points for β = 0,9

Figure 16 shows the load × displacements curve at the central point that has been obtained when the modified Von Mises elasto-plastic model was assumed at each concrete layer. Elastic responses were observed until the load factor reached β=0.43. The reinforcement yielded at central point for β=0.44, equivalent to the load of P=35,2Kips. The limit load, observed experimentally P=77kips, was computed by assuming ultimate plastic strain equal to 0.003, however the final deflection was rather smaller than the experimental value, w=0,72in. No concrete yielding has been observed in the compression zone.

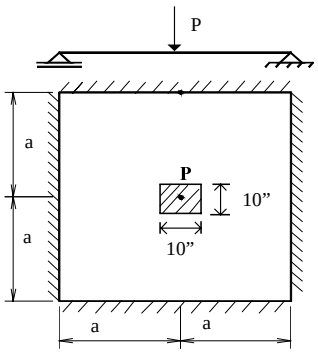

Figure 14 Plate definition

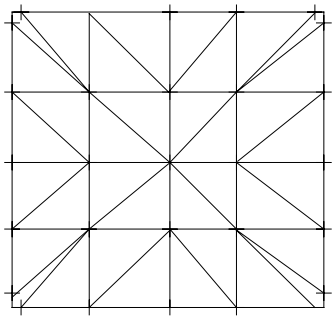

Figure 15. Plate discretization.

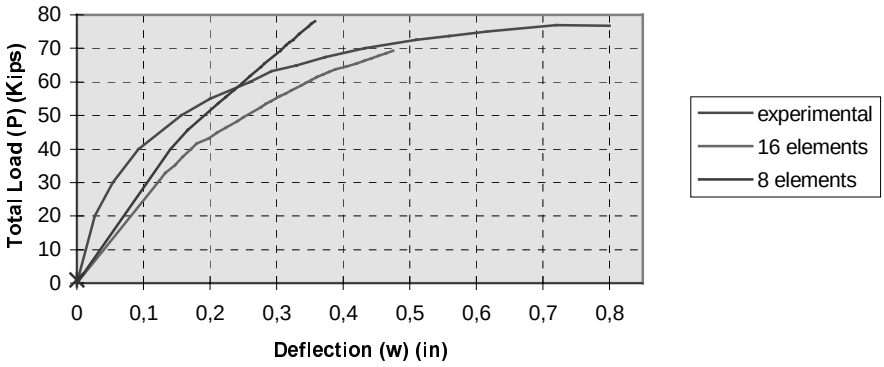

Figure 16. Load-deflection curve of the central point

The example was also analysed by assuming the concrete material governed by a damage model. The damage internal variable D was limited to 0.9, 0.85 and 0.8. The discretization adopted to analyse this case was only the course one described previously. The solution obtained, by applying the load in 48 increments, is illustrated in figure 18, where the central point load × displacement curve is displayed. For the case of limiting the damage to 0.8, the steel has yielded at a load equal to 46Kips, while the concrete largest strain 0.003 was reached when the applied load was 76.4kips. The accuracy of the integration scheme along the slab thickness has been tested using 4, 8 and 12 stations, giving the following ultimate loads and corresponding deflections: P=74,8kips, 76,4kips and 76,4kips; w=0,785in, w=0,817in and w=0,8in, respectively. They do not presented significant differences, therefore, as for the plastic case, 8 points seem to be a reasonable scheme, considering that the results obtained experimentally were P=77kips and w=0,8in. Figure 17 exhibits the results achieved by the Gauss point number cases taken to run this problem. The two station case has also been included, but as expected it reduces the wrongly the slab stiffness.

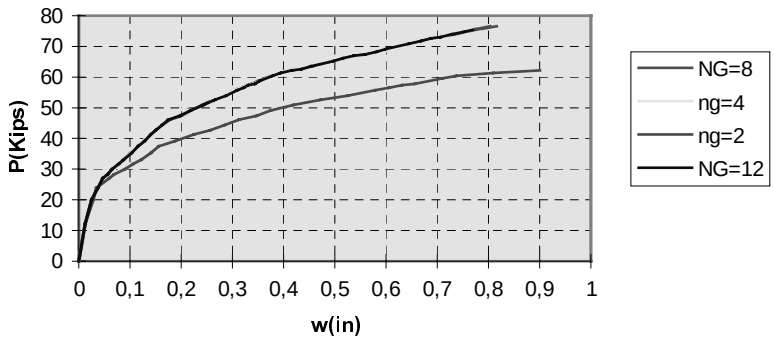

Figure 17. Load × Displacement curves varying the number of stations.

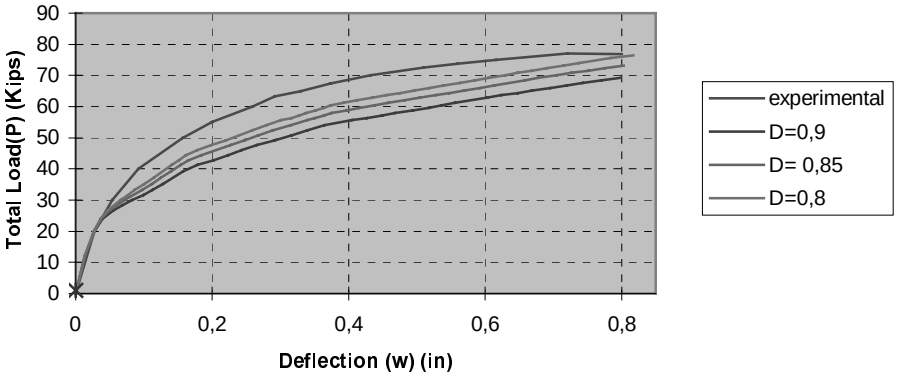

Figure 18: Load × Displacement curves varying the damage limit

7 CONCLUSIONS

A BEM formulation to deal with Kirchhoff's plate bending problems exhibiting thickness or stiffness variable and then extended to non-linear problems has been developed. The integral representations for this problems is derived from a particular reciprocity relation that can also be used to derive the standard formulation that consider an initial moment field. Two alternatives to take into account the stiffness variation have been discussed. The non-linear BEM formulation is also discussed, now assuming the plate subdivided into layers that exhibit different material behaviour. The developed technique is applied to analyse reinforced concrete slabs. The efficiency of all proposed models is illustrated by examples, that have shown good accuracy even when rather coarse discretization were adopted. Moreover, for the case of varying stiffness, the numerical solutions shown not to be too sensitive to internal discretizations, allowing therefore the use of domain coarse meshes with few internal points to lead to small matrix sizes, without loosing accuracy.

8 REFERENCES

1. Bezine, G.P., Boundary integral formulation for plate flexure with arbitrary boundary conditions, *Mech. Res. Comm*., 1978, 5 (4), 197-206.
2. Bezine, G.P. & Gambi, D.A., A new integral equation formulation for plate bending problems. In: *Recent advances in boundary element methods*, Brebbia, C.A. ed., Pentech Press, 1978
3. Stern, M.A., A general boundary integral formulation for the numerical solution of plate bending problems, *Int. J. Solids Struct*., 1979, 15, 769-782.
4. Tottenhan, H., The boundary element method for plates and shells. In: *Developments in boundary element methods*, Banerjee, P.K. & Butterfield, R. eds., 173-205, 1979.
5. Jaswon, M.A., Maiti, M.& Symm, G.T., Numerical biharmonic analysis and some applications. *Int. J. Solids & structures*, 3, 309-332, 1967.

6. Jaswon, M.A. & Maiti, M., An integral formulation of plate bending problems. *J. Eng. Math*., 2, 83-93, 1968.
7. Altiero, N.J. & Sikarskie, D.L., A boundary integral method applied to plates of arbitrary plan form. *Computer & Structures*, 9, 163-168, 1978.
8. Guo-Shu S. & Mukherjee S., Boundary element method analysis of bending of elastic plates of arbitrary shape with general boundary conditions, *Engineering Analysis with Boundary Elements*, 3, 36-44, 1986.
9. Hartmann, F.& Zotemantel, R., The direct boundary element method in plate bending, *Int. J. Num. Meth. Eng*., 23(11), 2049-2069, 1986.
10. Venturini, W.S. & Paiva, J.B., Boundary elements for plate bending analysis, *Engineering Analysis*, 11, 1-8, 1993.
11. Van Der Weeën, F. Application of the direct boundary element method to Reissner's plate model, In: *Boundary element methods in engineering*, Brebbia, C.A., ed., Springer-Verlag, 1982.
12. Reissner, E. The effect of transverse shear deformation on the bending of elastic plates. *Journal of applied Mechanics*, 12, A69-A77, 1945.
13. Tanaka, M., Large deflection analysis of thin elastic plates. In: *Developments in boundary element methods - 3*, Banerjee, P.K. & Butterfield, R. eds., 1984.
14. Kamiya, N. & Sawarky, Y., An integral equation approach to finite deflection of elastic plates. *Int. J. Non-linear Mechanics*, 17, 187-194, 1982.
15. Telles, J.C.F. & Brebbia, C.A. On the application of the boundary element method to plasticity. *Appl. Math. Modelling*, 3, 466-470,1980.
16. Moshaiov, A. & Vorus, W.S., Elasto-plastic plate bending analysis by a boundary element method with internal initial plastic moments, *Int. J. Solids & Structures*, 22, 1213-1229, 1986.
17. Chueiri, L.H.M.& Venturini, W.V., Elastoplastic BEM to model concrete slabs. In: *Boundary Elements XVII*, Brebbia, C.A. et all. eds., Computational Mechanics Publications, Southampton, 1995.
18. Ribeiro, G.O. & Venturini, W.S. Boundary element formulation for non-linear problems using the Reissner's theory, *Proc. of the Sixth Boundary Element Technology Conference*, C.A. Brebbia ed., Computational Mechanics Publications, Southampton, U.K., 239-251, 1991.
19. Karan, V.J & Telles, J.C.F., The BEM applied to plate bending elastoplastic analysis using Reissner's theory. *Engineering Analysis with Boundary Elements*, 9, 351-357, 1992.
20. Aliabadi, M.H.ed., *Boundary element method for plate bending analysis*. Southampton, CMP, 1998.
21. CEB-FIP, Model code *1990 (MC -90), bulletin D'Information*, n.195,196 and 198, 1990.
22. S. Timoshenko, and S. Woinowsky-Krieger, *Theory of plates and shells*. New York, McGraw-Hill, 1959.
23. F.R. Hand, D.A Pecknold and W.C. Schnobrich, Nonlinear layered analysis of RC plates and shells. *J. Struct. Div. ASCE*, 99, ST7, 1491-1505 (1973)
24. J.A. Figueiras, *Ultimate load analysis of anisotropic and reinforced concrete plates and shells*. Ph.D. thesis, University College of Swansea (1983)

25. H.B. Kupfer, and K.H. Gerstle, Behaviour of concrete under biaxial stresses. *Eng. Mech. Div., ASCE*, 99 (1973).
26. J.L., Batoz, K.J. Bathe, and L. H. Wong, A study of three-node triangular plate bending elements. *Int. J. Num. Meth. Eng*., 15, 1771-1812 (1980).
27. J.A. Mazars, *Application de la mécanique de l'endommagement au comportement nonlinéare et à la rupture du béton de structure*. Dr of Science thesis. University of Paris 6, 1984.
28. J.A. Mazars, description of micro and macroscale damage of concrete structures. *Eng. Fracture Mechanics*, v.25, 1986.

APPENDIX

The displacement fundamental value computed at the field point q due to an unit load applied at the source point, is expressed by,

$$w^*(s,q) = r^2(\ell nr - 1/2)/(8\pi D_o) \tag{A.1}$$

where r = r(s,q) is the distance between the points s and q, and D_o is a reference plate stiffness taken, for convenience, equal to the source point stiffness D(s).

By differentiating equation (A.1) and applying the appropriate definitions one can find the other required fundamental values:

$$\frac{\partial w^*}{\partial n} = \frac{r}{4\pi D_o}\ln(r)\left(r_{,i}\, n_i\right) \tag{A.2}$$

$$M_n^* = -\frac{1}{4\pi}\left[(1+\nu)\ln(r) + (1-\nu)\left(r_{,i}\, n_i\right)^2 + \nu\right] \tag{A.3}$$

$$M_{ns}^* = -\frac{1}{4\pi}(1-\nu)\left(r_{,i}\, n_i\right)\left(r_{,j}\, s_j\right) \tag{A.4}$$

$$V_n^* = \frac{r_{,i}\, n_i}{4\pi r}\left[2(1-\nu)\left(r_{,j}\, s_j\right)^2 - 3 + \nu\right] + \frac{1-\nu}{4\pi R}\left[1 - 2\left(r_{,i}\, s_i\right)^2\right] \tag{A.5}$$

$$R_C^* = M_{ns}^{*+} - M_{ns}^{*-} \tag{A.6}$$

where n and s represents the outward and tangent unit vectors, respectively, and the superscripts + and - are used to indicate values taken before and after the corner.

All kernels found when deriving moment and shear force representations, equations (11) and (12), are easily computed following the effort definitions, equations (3) and (4). For a symbolic fundamental value F^* the kernels $\overline{M}_{nij}^*$, $\overline{M}_{nsij}^*$, $\overline{V}_{nij}^*$ and $\overline{R}_{Cij}^*$ are given by the expression:

$$\overline{F}_{ij}^*(s,Q) = -\left(\nu\delta_{ij}\frac{\partial^2 F^*}{\partial x_v \partial x_v}(s,Q) + (1-\nu)\frac{\partial^2 F^*}{\partial x_i \partial x_j}(s,Q)\right) \tag{A.7}$$

Similarly, the kernels appearing in equation (12) are given by,

$$\overline{F}_i^*(s,Q) = -\frac{\partial}{\partial x_i}\left(\frac{\partial^2 F^*}{\partial x_k \partial x_k}(s,Q)\right) \tag{A.8}$$

The remaining kernels in both equations w_{ij}^*, w_i^*, w_{Cij}^* and w_{Ci}^* are directly obtained from the fundamental value w^*, assuming the stiffness D equal the unit and applying formulas (A.7) and (A.8). Their final expressions can be conveniently derived the following operators:

$$w_{ij}^*(s,Q) = -\left(\nu\delta_{ij}\frac{\partial^2 w^*}{\partial x_v \partial x_v}(s,Q) + (1-\nu)\frac{\partial^2 w^*}{\partial x_i \partial x_j}(s,Q)\right) \tag{A.9}$$

$$w_i^*(s,Q) = \frac{\partial}{\partial x_i}\left(\frac{\partial^2 w^*}{\partial x_k \partial x_k}(s,Q)\right) = \frac{-r_{,i}}{2\pi r} \tag{A.10}$$

The kernels present in the initial moment integral representations, equations (13) and (14), can be easily derived using the second and third derivatives of the fundamental values $V_n^*(s,Q)$, $M_n^*(s,Q)$, $R_C^*(s,C)$, $w_C^*(s,C)$, $w^*(s,Q)$, $\partial w^*(s,Q)/\partial n$ and $w_{,k\ell}^*(s,q)$, applying the operator (A.9) and (A.10), now multiplied by the source point stiffness D(s).

The free term of equation (13), appeared due to the differentiation of a singular integral, is given by,

$$g_{ijk\ell}(s) = -\tfrac{1}{8}\left[(1-\nu)(\delta_{ik}\delta_{\ell j} + \delta_{kj}\delta_{i\ell}) + (1+3\nu)\delta_{ij}\delta_{k\ell}\right] \tag{A.11}$$